# Rotatable anisotropy and coercivity in exchange-bias bilayers

J. Geshev,* L. G. Pereira, and J. E. Schmidt
*Instituto de Física–UFRGS, Caixa Postal 15051, 91501-970, Porto Alegre, RS, Brazil*
(Received 23 April 2002; revised manuscript received 27 June 2002; published 31 October 2002)

A phenomenological approach for polycrystalline exchange-bias bilayers is proposed which explains the coercivity enhancement as well as its temperature and coupling strength dependences. In the model, it is assumed that uncompensated interfacial antiferromagnetic grains can switch their magnetizations irreversibly, producing a rotatable anisotropy. A preferential distribution of the antiferromagnetic easy axes is also considered. An inhomogeneous ferromagnetic magnetization reversal is allowed, assuming that the ferromagnet is divided into domains, each coupled to a stable antiferromagnetic grain only. The antiferromagnetic anisotropy distribution affects the angular dependence of the coercivity, reducing its value in the vicinity of the exchange-bias direction, also smoothing the loop shift variations, more notably for small ferromagnetic uniaxial anisotropy. The inclusion of the rotatable anisotropy changes the shape of the magnetization curves and their characteristics. The larger the relative contribution of the rotatable anisotropy to the effective uniaxial anisotropy, the closer the loop shift angular variation gets to a pure cosine behavior, and no significant effect on the coercivity for strong coupling is detected. The frequently observed peak in the temperature variation of the coercivity is also explained considering the variation of the rotatable anisotropy, which is directly connected to the temperature dependence of the unstable antiferromagnetic grains' magnetization.

DOI: 10.1103/PhysRevB.66.134432 PACS number(s): 75.70.Cn, 75.30.Gw, 71.70.Gm, 75.60.−d

## I. INTRODUCTION

Exchange interactions at the interface between ferromagnetic (FM) and antiferromagnetic (AF) materials, responsible for the exchange-bias phenomenon,[1,2] even though discovered almost five decades ago, still receive considerable attention (recent reviews can be found in Refs. 3–5). No doubt, to a great extent, this is due to the important technological application the exchange bias has found in information storage technology.[6,7] Other reasons include the following: (i) despite the fact that most of the existent models[8–19] quantitatively explain the best known macroscopic magnetic property of the exchange anisotropy, the hysteresis loop shift field $H_{eb}$, the enhancement of the coercivity, $H_c$, when compared to that of an uncoupled film, is less well understood (such an enhancement has also been observed in mechanically alloyed AF/FM powders[20]); (ii) the observation of a negative isotropic shift in the ferromagnetic resonance (FMR) field in exchange-bias films;[21–23] and (iii) the fact that different experimental techniques may yield different values for the exchange-bias field.[21,24–30] These differences, at least in some cases, could be assigned either to the fact that the measurements are performed on different sets of samples,[28] or because the model used to interpret the experimental data from reversible measurement techniques may not be very plausible.[29]A recent study of our group[30] showed that the $H_{eb}$ values derived from FMR and hysteresis loop measurements are different physical entities and, in general, must give different values, because there are different magnetization processes involved in the corresponding measurements.

Several possible explanations for the increased coercivity have been proposed. One includes a random field at the FM/AF interface that results in formation of domains in the FM layer, incorporated by Li and Zhang,[16] where the enhancement of $H_c$ is attributed to effective lateral domain-wall pinning in the FM layer by AF domain perpendicular to the interface. Qian *et al.*,[12] on the other hand, introduced an uniaxial interfacial anisotropy in order to explain the coercivity enhancement, and Leighton *et al.*[17] proposed that interfacial magnetic frustration provides local energy minima which pin the propagating domain walls in the ferromagnet, leading to an enhanced coercivity.

Phenomenological approaches that explain both the isotropic negative FMR shift and the increased coercivity in exchange-coupled bilayers with polycrystalline AF layer were proposed in the Fulcomer and Charap model[8] (FC model) and in the Stiles and McMichael model[13] (SM model). In both models the basic assumption is that there must be two parts in the AF layer, one with ''rotatable''[31] anisotropy and another with ''nonrotatable'' anisotropy. The FC model treats the thermal behavior of the system of AF grains of uniform orientation and uniform magnetization, where the barrier to reversal is determined by a volume anisotropy. This model seems to be a good approximation for very small AF grains. In the SM model, the AF grains are randomly oriented and have partial domain walls. For larger grains, where the barrier to reversal is determined by a domain-wall energy, the SM model is likely to be a better approximation. This model also includes inhomogeneous reversal as an additional mechanism for the increased coercivity, which contributes to the coercivity at all temperatures.

The frequently observed FMR field shift has been explained[8,21] in terms of a rotatable anisotropy field $H_{\mathrm{ra}}$, a field that in FMR measurements rotates to be parallel to the equilibrium direction of the FM magnetization. At a given temperature $T$, the magnetizations of the smaller grains are oriented along the applied field **H**, thus producing the rotatable anisotropy sensed by the ferromagnetic film. The larger grains, however, remain pinned to the cooling field (if the sample is cooled in a magnetic field in order to produce the exchange-bias state) or to the field applied during the bilayer's deposition, thus producing the unidirectional anisotropy.

 

In the present paper we calculate the angular dependences of the exchange-bias field shift and coercivity derived from hysteresis loop measurements in FM/AF bilayers in the framework of a phenomenological model that takes into account both rotatable and nonrotatable contributions to the AF layer anisotropy. The influence of the AF easy-axis distribution on the bias field and coercivity has also been discussed, as well as the variations of the coercivity with the exchange interaction field strength and its temperature dependence.

## II. MODEL

We model a FM film with magnetization vector $\mathbf{M_{FM}}$ coupled to a polycrystalline AF film consisting of large (stable) AF grains, which contribute to the unidirectional anisotropy, as well as of small (unstable) AF grains. The latter, due to the exchange interaction with the FM magnetization, can irreversibly change their magnetization directions, thus producing effective rotatable anisotropy. Possible mechanisms for this anisotropy can be irreversible domain-wall motion[21] or thermal instability, i.e., a superparamagneticlike behavior, as assumed by Fulcomer and Charap.[8] The AF magnetizations have uniaxial anisotropy and, due to the weakness of the Zeeman term, are coupled to the FM magnetization only. If the easy axes of the large AF grains are parallel to each other, we assume that all FM spins rotate coherently. However, preferential (and not random, as supposed in the SM model) distribution of the AF easy-axis directions in the plane of the film can also be considered.[18,19] In-plane anisotropic macrostress or a textured structure, e.g., can give rise to a preferentially distributed AF anisotropy. In such a case, it is accepted here that the FM film is divided into domains, each coupled to a stable AF grain only; thus the FM reversal could be inhomogeneous, as is also assumed in the SM model. Such an assumption is supported by the results of Nolting *et al.*,[32] which implies that the spin alignment in individual FM domains close to the interface is determined, domain by domain, by the spin directions in the adjacent AF grains.

The total free energy per unit area of a FM domain coupled to a stable AF grain magnetization can be written as

$$E = E_{\mathrm{FM}} + E_{\mathrm{AF}} + E_{\mathrm{int}}. \tag{1}$$

The FM domain wall energy in this equation, normalized to the FM layer thickness, $t_{\mathrm{FM}}$, is

$$\frac{E_{\mathrm{FM}}}{t_{\mathrm{FM}}} = 2\pi(\mathbf{M_{FM}}\cdot\hat{\mathbf{n}})^2 - \mathbf{H}\cdot\mathbf{M_{FM}} - K_{\mathrm{FM}}\left(\frac{\mathbf{M_{FM}}\cdot\hat{\mathbf{u}}_{\mathbf{FM}}}{M_{\mathrm{FM}}}\right)^2 - K_{\mathrm{ra}}\left(\frac{\mathbf{M_{FM}}\cdot\hat{\mathbf{h}}}{M_{\mathrm{FM}}}\right)^2, \tag{2}$$

where the first three terms are the demagnetizing, the Zeeman, and the FM uniaxial anisotropy energies, respectively. Note that in the SM model it is assumed that there is no anisotropy in the ferromagnet except the anisotropy induced by the coupling to the AF grains. Here we accept that a part of the uniaxial anisotropy, the one with anisotropy constant $K_{\mathrm{FM}}$, could be intrinsic to the FM layer; many single FM layered samples present such an anisotropy. The unit vectors $\hat{\mathbf{u}}_{\mathbf{FM}}$, $\hat{\mathbf{n}}$, and $\hat{\mathbf{h}}$ represent the FM layer uniaxial anisotropy direction, the normal to the film surface direction, and the applied field direction, respectively. (Although it is not done in the present work, cubic magnetocrystalline anisotropy energy should also be included in the above energy form when necessary.)

The last term in Eq. (2) refers to the rotatable anisotropy. McMichael *et al.*[21] included a unidirectional rotatable anisotropy term of a form $-\mathbf{M_{FM}}\cdot\mathbf{H}_{\mathrm{ra}}$ in the AF part of the anisotropy energy in their work concerning the isotropic FMR shift. Note that this energy could equally well be uniaxial anisotropy of the FM layer with a constant $K_{\mathrm{ra}}$, with a symmetry axis along the applied field direction,[31,33] as will be considered here. Rotatable anisotropy of such a form should be used to model irreversible magnetization processes, where the directions of $\mathbf{M_{FM}}$ and $\mathbf{H}$ may differ considerably.

It is worth noting that when two uniaxial anisotropies (in the case into consideration with constants $K_{\mathrm{FM}}$ and $K_{\mathrm{ra}}$) are present together with easy axes at some angle to each other, rather than at right angle, they are equivalent to a new uniaxial anisotropy.[34] The direction of this new axis is determined by the ratio between $K_{\mathrm{FM}}$ and $K_{\mathrm{ra}}$, i.e., lies closer to $\hat{\mathbf{u}}_{\mathbf{FM}}$ direction if $K_{\mathrm{FM}} > K_{\mathrm{ra}}$, and has a strength higher than $K_{\mathrm{FM}}$. When $K_{\mathrm{FM}} = K_{\mathrm{ra}}$, this axis lies midway between $\hat{\mathbf{u}}_{\mathbf{FM}}$ and $\hat{\mathbf{h}}$ directions, and has a strength equal to $K_{\mathrm{FM}}$. If the axes are at right angles, the new direction of easiest magnetization is the one of the axis with higher anisotropy constant. Thus, as the applied field is rotated from the exchange-bias direction, the resultant FM uniaxial anisotropy axis is rotated as well, and its direction is determined by the $K_{\mathrm{FM}}/K_{\mathrm{ra}}$ ratio.

The second term in Eq. (1) accounts for the energy of a stable AF grain with magnetization $\mathbf{M_{AF}}$, which here will be considered to be either the energy required to reversibly form domain wall at the AF side of the interface as the FM magnetization is rotated,[10]

$$E_{\mathrm{AF}}^{\mathrm{W}} = -\sigma_{\mathrm{W}}\frac{\mathbf{M_{AF}}\cdot\hat{\mathbf{u}}_{\mathbf{AF}}}{M_{\mathrm{AF}}} \tag{3}$$

(where $\sigma_{\mathrm{W}}$ is the energy per unit surface of a 90° domain wall), or the uniaxial anisotropy energy of such a grain with anisotropy constant $K_{\mathrm{AF}}$ and easy-axis direction given by the unit vector $\hat{\mathbf{u}}_{\mathbf{AF}}$,

$$\frac{E_{\mathrm{AF}}^{u}}{t_{\mathrm{AF}}} = -K_{\mathrm{AF}}\left(\frac{\mathbf{M_{AF}}\cdot\hat{\mathbf{u}}_{\mathbf{AF}}}{M_{\mathrm{AF}}}\right)^2, \tag{4}$$

where $t_{\mathrm{AF}}$ is the thickness of the AF grain. Note that formation of a planar domain wall in the AF grain does not result in formation of a domain wall in the adjacent ferromagnet: the AF domain wall is formed parallel to the interface, and the FM moment senses only the interfacial moment of the adjacent AF grain.[10]

The last term in Eq. (1) represents the interaction energy. The two contributions to $E_{\mathrm{int}}$ which can be considered are the direct coupling to the net moment of the AF grain, $J_1$, ($J_1 > 0$ and $J_1 < 0$ correspond to ferromagnetic and antiferro-

magnetic couplings, respectively), and the spin-flip coupling, $J_2$, which favors a perpendicular relative orientation between the FM and AF moments:

$$E_{\rm int} = -J_1 \frac{\mathbf{M_{FM}} \cdot \mathbf{M_{AF}}}{M_{\rm FM} M_{\rm AF}} + J_2 \left( \frac{\mathbf{M_{FM}} \cdot \mathbf{M_{AF}}}{M_{\rm FM} M_{\rm AF}} \right)^2 . \qquad (5)$$

Note that if $K_{\rm ra}=0$, $J_2=0$, $\hat{\mathbf{u}}_{\mathbf{FM}} \| \hat{\mathbf{u}}_{\mathbf{AF}}$, and if the expression given in Eq. (3) is used for $E_{\rm AF}$, the present model reduces to that of Mauri *et al.*[10] In what follows, we refer to this model as the DWF (i.e., domain-wall formation) model. When $K_{\rm ra} \neq 0$, the corresponding abbreviation will be DWFra. Also, when Eq. (4) is used for the AF anisotropy energy, our model is reduced to that of Meiklejohn.[2] Moreover, if in the latter model $K_{\rm AF}$ (or $\sigma_{\rm W}$ in the DWF model) value is very high, then the AF moment will be fixed along its easy-axis direction, and we will have a model identical to that of Xi and White,[35] abbreviated as the FAF (fixed AF moment) model. The corresponding abbreviation for the case when $K_{\rm ra} \neq 0$ will be FAFra. In Sec. III hysteresis loops are computed for several representative cases, for coherent and inhomogeneous FM reversals.

The static equilibrium directions of $\mathbf{M_{FM}}$ and $\mathbf{M_{AF}}$ can be calculated from Eq. (1) by finding the polar ($\theta_{\rm FM}$ and $\theta_{\rm AF}$) and azimuthal ($\phi_{\rm FM}$ and $\phi_{\rm AF}$) angles of $\mathbf{M_{FM}}$ and $\mathbf{M_{AF}}$ in the spherical coordinate system for which $E$ is at minimum. The projections of $\mathbf{M_{FM}}$ and $\mathbf{M_{AF}}$ along the field direction will give the magnetizations of the layers (or grains). The energy minimization procedure used here is established in our previous works.[29,30]

## III. RESULTS AND DISCUSSION

In this section, calculations of complete hysteresis loops, the angular dependence of the hysteresis loop shift field and the coercivity, as well as variations of the coercivity with the exchange interaction field strength and with the temperature, are presented and discussed. Perpendicular or spin-flop coupling have not been considered, i.e., $J_2=0$ for all calculations.

### A. Hysteresis loop calculations

Magnetization curves have been calculated for various values of the effective fields, which are: the uniaxial FM anisotropy field, $H_{\rm U}=2K_{\rm FM}/M_{\rm FM}$, the domain wall field, $H_{\rm W}=\sigma_{\rm W}/(t_{\rm FM}M_{\rm FM})$, the interface coupling field, $H_{\rm E}=J_1/(t_{\rm FM}M_{\rm FM})$, and the rotatable anisotropy field $H_{\rm ra}=2K_{\rm ra}/(t_{\rm FM}M_{\rm FM})$. As the number of effective fields is quite large, it was not possible here, unfortunately, to consider all possible combinations of these parameters. Taking this into account, we used a limited number of parameter sets in the calculations, trying to cover the most feasible cases. That is, we do not claim that our choices were systematic; the criteria were, in most of the cases, the similarity of the calculated curves to experimentally measured ones. We believe, however, that the conclusions drawn in the present paper are valid for the majority of the practicable parameter combinations.

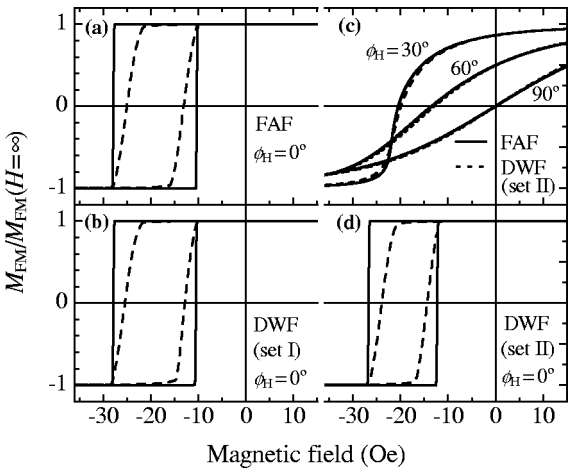


FIG. 1. Hysteresis loops for $\phi_{\rm H}=0°$ calculated using (a) the FAF model ($H_{\rm U}=9.16$ Oe, $H_{\rm E}=19.1$ Oe), (b) the DWF model (set I: $H_{\rm U}=12.8$ Oe, $H_{\rm W}=100$ Oe, $H_{\rm E}=18.6$ Oe), and (c) magnetization curves for three field directions for the set of parameters used in panel (a) for the FAF model (solid curves), and for the parameters used in panel (d) for the DWF model (dots). (d) Hysteresis loops calculated via the DWF model for another set of parameters (set II: $H_{\rm U}=8$ Oe, $H_{\rm W}=1.2$ kOe, $H_{\rm E}=19.2$ Oe). The dashed curves in panels (a), (b), and (d) correspond to Gaussian AF easy-axis direction distributions with maxima at the exchange-bias direction and a standard deviation $\sigma=5°$.

In the present study, the magnetic field is applied in the film's plane and characterized by its azimuthal angle $\phi_{\rm H}$, i.e., the angle between the positive field direction and $\hat{\mathbf{u}}_{\mathbf{FM}}$; the latter, as well as $\hat{\mathbf{u}}_{\mathbf{AF}}$, also lies in the plane of the film.

In order to compare our calculations with previous experimental and model results, we initially employed the parameters from the work of Xi and White ($H_{\rm U}=9.16$ Oe and $H_{\rm E}=19.1$ Oe), used there to fit experimental data for NiFe/CrMnPt bilayers.[35] The corresponding hysteresis loop for $\phi_{\rm H}=0°$, calculated via the FAF model, is shown in Fig. 1(a). The hysteresis loop given by the solid curve in panel (b) was calculated here in the framework of the DWF model (set I: $H_{\rm U}=12.8$ Oe, $H_{\rm W}=100$ Oe, $H_{\rm E}=18.6$ Oe). It can be seen that the solid curves in panels (a) and (b) (which although are in very good agreement with the above cited $H_{eb}$ experimental data, do not fit neither $H_c$ value nor the hysteresis loop shape), are practically identical. The dashed curves in panels (a), (b), and (d) are the corresponding hysteresis loops where a normal (Gaussian) distribution of the AF easy-axis directions is assumed with maximum at the exchange-bias direction and standard deviation $\sigma=5°$ and maximum deviation of 11°. In these calculations, 221 individual magnetization curves (corresponding to each of the AF grain easy-axis directions) were obtained for each $\phi_{\rm H}$ by minimizing Eq. (1) when $H$ is varied. This results in rounded hysteresis loops, each of them being a weighted average curve of the above 221 curves.

The solid curves in Fig. 1(c) represent the calculated magnetization curves for $\phi_{\rm H}=30°$, 60° and 90° for the above cited set of parameters for the FAF model, which fit very well the corresponding experimental data reported in Ref. 35

(this FAF set, however, did not fit the shape of the loop and the $H_{eb}$ value for $\phi_H=0°$ well, as mentioned above). The dotted curves in the same figure have been obtained using the DWF model and a parameter set which is different from the one used to calculate the curves in panel (b) (set II: $H_U=8$ Oe, $H_W=1200$ Oe, $H_E=19.2$ Oe). Once again, the fitting curves obtained using the two distinct models are practically identical. For reference purposes, in panel (d) we plot the hysteresis loop for $\phi_H=0°$ obtained using the parameter set II (solid curve); the loop calculated using the distribution of AF easy-axis directions is plotted as well. One can observe that the loop shift is equal to that of the curves shown in panels (a) and (b); however, the coercivity value is smaller, and the dashed curve represents a better fit to the experimental data of Xi and White than the one obtained via the FAF model. This is not surprising having in mind that the DWF model is more flexible than the FAF one; actually, as already mentioned above, the latter is a special case of the DWF model when $\sigma_W=\infty$. Our numerical results, using the DWF model and AF easy-axis direction distribution, are similar to those of Stiles and McMichael,[13] who also compared their model curves to the Xi and White experimental results.

As follows from Eq. (2), for $\phi_H=0°$, the inclusion of a nonzero rotatable anisotropy does not change the calculated loops if the value of the effective uniaxial anisotropy along the exchange-bias direction, $H_U+H_{ra}$, is kept fixed while $H_{ra}$ is increased. When $\phi_H\neq 0°$, however, the shape of the magnetization curves as well as the $H_{eb}$ and $H_c$ values change. Figure 2 shows representative magnetization curves calculated for $\phi_H=20°$ through the DWFra model for various ratios between $H_E$ and $H_W$, maintaining $H_U+H_{ra}$ constant, i.e., either 5 Oe for panels (a)–(c) or 80 Oe for panels (d)–(f). The curves for the cases of $H_{ra}=0$, $H_{ra}=H_U$, and $H_U=0$ are demonstrated. The curves corresponding to the FAFra model (not shown) are very similar to the ones for a high $H_W$ value plotted in panel (f), as expected.

When the $H_U+H_{ra}$ value is small compared to $H_E$, the relative increase of $H_{ra}$ leads to a more rapid magnetization change in second and third quadrants, bringing along a monotonic decrease of $H_{eb}$ for all $H_W$, see Figs. 2(a)–(c). For higher $H_U+H_{ra}$ values, however, neither $H_{eb}$ nor $H_c$ variations with $H_{ra}$ are simple, as can be seen in panels (d)–(f) of the same figure. In order to shed light on this question, a series of hysteresis loops has been calculated for a number of parameter sets $(H_U,H_W)$ for $H_E=20$ Oe and $\phi_H=20°$. The corresponding dependencies of $H_{eb}$ and $H_c$ on the relative $H_{ra}$ contribution to the FM anisotropy are plotted in Fig. 3 for two cases, $H_U+H_{ra}=H_E$ and $H_U+H_{ra}=4\,H_E$. Only when the AF anisotropy is strong ($H_W=1200$ Oe) and for small effective FM anisotropy [panel (a)] are the $H_{eb}$ and $H_c$ variations monotonic. In all other cases, there is a maximum [local one for panel (a)] and a minimum in each $H_c$ dependence. The corresponding $H_{eb}$ variations also show maxima for the same relative $H_{ra}$ values where $H_c$'s are maxima. Note that $H_{eb}$ can even change its sign: when $H_W=H_E$ [the dashed curve in panel (b)], $H_{eb}$ is positive for $H_{ra}/(H_U+H_{ra})<0.3$ and negative in the rest of the interval. It should be emphasized here that the above effect must not be confounded with the positive exchange bias effect,[37] whose explanation is based on the existence of an AF coupling at the FM/AF interface.

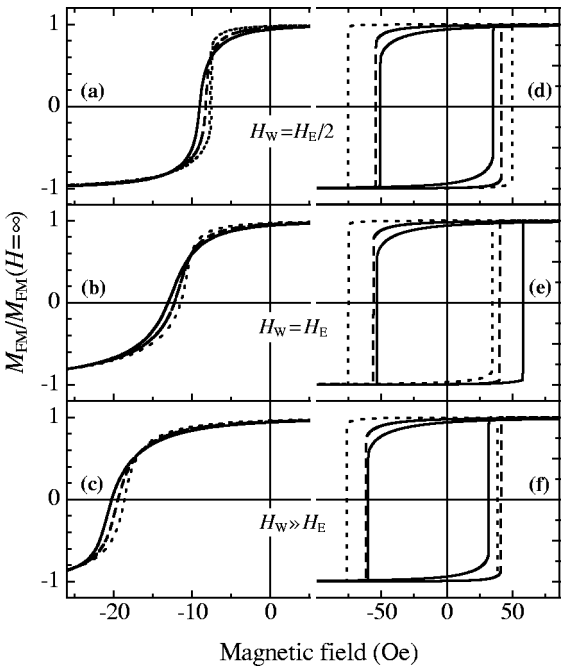


FIG. 2. Magnetization curves calculated via the DWF model for $\phi_H=20°$ and $H_E=20$ Oe, where $H_W=10$ Oe in panels (a) and (d), $H_W=H_E$ in panels (b) and (e), and $H_W=1.2$ kOe in panels (c) and (f). $H_U+H_{ra}$ is maintained equal to 5 Oe in panels (a)–(c), and equal to 80 Oe in panels (d)–(f), where the solid, dashed and dotted curves represent the cases of $H_{ra}=0$, $H_U=H_{ra}$, and $H_U=0$, respectively.

### B. Angular dependences of $H_{eb}$ and $H_c$

As seen in Fig. 1, because there are enough unknown parameters, it is possible to fit well any particular experimental data by using different models when **H** is applied along certain direction [or several directions; see Fig. 1(c)]. In or-

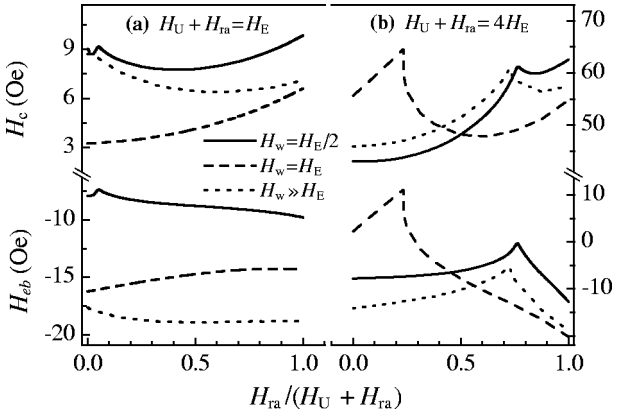


FIG. 3. $H_{eb}$ and $H_c$ vs $H_{ra}/(H_U+H_{ra})$ for $H_W=20$ Oe and $\phi_H=20°$ obtained via the DWFra model. (a) $H_U+H_{ra}=20$ Oe. (b) $H_U+H_{ra}=80$ Oe.

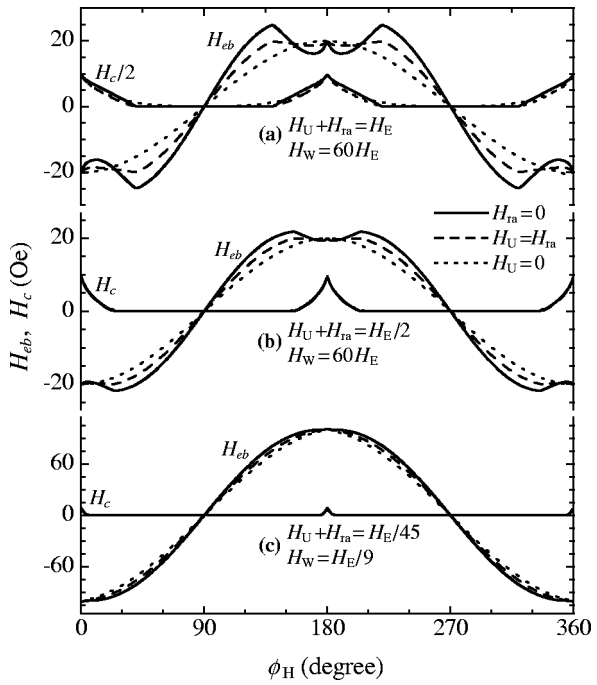


FIG. 4. Angular dependence of $H_{eb}$ and $H_c$ for $H_E=20$ Oe in panels (a) and (b), and $H_E=900$ Oe for panel (c) obtained through the DWFra model. $H_U+H_{ra}$ is kept fixed at 20 Oe in panels (a) and (c), and 10 Oe in panel (b).

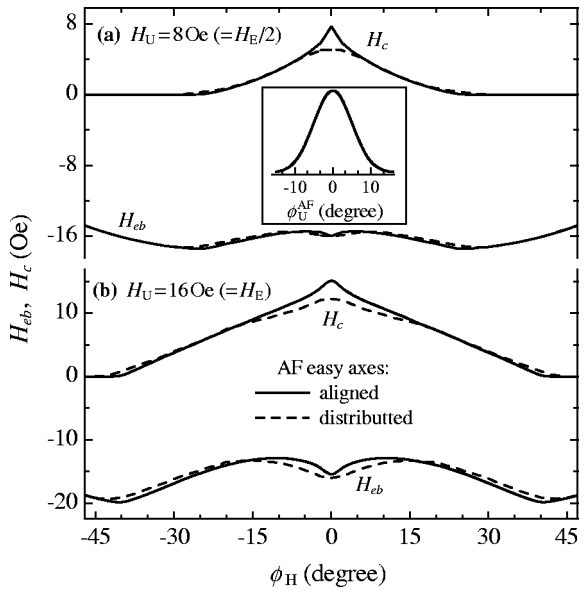


FIG. 5. Influence of the AF easy-axis distribution on the angular dependences of $H_{eb}$ and $H_c$ for $H_E=20$ Oe, $H_W=1.2$ kOe, and $H_{ra}=0$, derived from magnetization curves calculated via the DWFra model. (a) $H_U=8$ Oe. (b) $H_U=16$ Oe. The solid curves are for the case of all AF grains having the easy axis direction of the FM layer, and the dashed ones are for the case of the Gaussian distribution of the AF easy axis directions (denoted by the angles $\phi_U^{AF}$) with standard deviation $\sigma=5°$, given in the inset.

der to clarify the magnetization reversal mechanism and to provide another try-out for the validity of the theoretical model used, the latter should be tested to fit the dependence of $H_{eb}$ and $H_c$ on the applied field direction. One of the goals of the present study was to estimate how the rotatable anisotropy and the AF easy-axis direction distribution affect the above angular dependences.

#### *1. Rotatable anisotropy effects*

Varying the angle $\phi_H$ from 0 to $2\pi$, hysteresis loops have been calculated through the DWFra model for each $\phi_H$ for a number of parameter sets ($H_U+H_{ra}$, $H_W$, $H_E$). Representative angular dependencies of $H_{eb}$ and $H_c$, extracted from each loop, are plotted in Fig. 4, where $H_E$ was kept fixed in each panel, i.e., 20 Oe for panels (a) and (b), and 900 Oe for panel (c). As in Fig. 2, the value of $H_U+H_{ra}$ has been kept fixed while $H_{ra}$ is varied. For the range of parameters considered here, the relative increase of the rotatable anisotropy makes the $H_{eb}$ vs $\phi_H$ curves smoother for strong AF anisotropy, i.e., high $H_W$ values compared to those of $H_U$ and $H_E$ [panels (a) and (b)]. The $H_{eb}$ variation for this case become very close to a pure $\cos 2\phi_H$ behavior. For strong exchange coupling field strength, panel (c) in this figure, even the total substitution of $H_U$ by $H_{ra}$ has practically no effect on $H_{eb}$. The rotatable anisotropy does almost not affect the coercivity for the parameter sets used in panels (b) and (c). Keeping $H_W$ high and increasing $H_U+H_{ra}$ [panel (a)], one obtains smoother $H_c$ dependences with the relative increase of the rotatable anisotropy. For even higher $H_U+H_{ra}$ values (the corresponding curves are not shown here), the coercivity dependence is similar to that of panel (a), but does not go to zero away from the exchange-bias direction. This behavior is consistent with the experimental results of Dimitrov *et al.*[36] and of Ambrose, Sommer, and Chien.[38] It is also worth noting that the angular variations of $H_{eb}$ and $H_c$ for $H_{ra}=0$, plotted in panel (a) of Fig. 4, are very similar to those obtained experimentally by Gökemeijer, Ambrose, and Chien,[39] and that the curves given in panel (b) are consistent with the results of Xi and White.[35]

The effect of $H_{ra}$ on the $H_{eb}$ variation for a high effective uniaxial anisotropy is the same as that shown in Fig. 4(a). The relative increase of the rotatable anisotropy changes the shape of the $H_{eb}$ vs $\phi_H$ curves in a way similar to that caused by the increase of the exchange coupling strength.[30]

It must be emphasized that the value of the rotatable anisotropy field, obtained from magnetization curve fittings, could be different from the value estimated by fitting the corresponding FMR spectra which show isotropic resonance field shift.[21,23] One possible reason for this discrepancy is that the $H_{ra}$ could be frequency dependent as found in amorphous spin glass alloys.[33]

#### *2. Influence of the AF easy-axis distribution*

The effects of the distribution of the easy axes of the AF grains contributing to the exchange bias, i.e., the large AF grains, on the angular dependences of $H_{eb}$ and $H_c$ can be estimated from Fig. 5. In this figure, representative curves (for the $\phi_H$ range where differences between the curves can be noted) are plotted for two cases, $H_U=H_E/2$, given in panel (a), and $H_U=H_E$ [panel (b)], for strong AF anisotropy calculated via the DWF model. The solid curves show the

$H_{eb}$ and $H_c$ vs $\phi_H$ assuming that all AF grains have the same easy axis direction, the one of the FM layer. The dashed curves represent the case when the Gaussian AF easy axis distribution used in Fig. 1 is considered, which is also shown in the inset of Fig. 5. The consequences of the inclusion of preferentially distributed AF anisotropy is a reduction of the coercivity in the vicinity of the exchange-bias direction, resulting in rounded $H_c$ curves and smoother $H_{eb}$ curves. This decrease of the $H_c$ values is more pronounced for small uniaxial anisotropy, being of the order of 35% for $\phi_H=0$ [panel (a) in Fig. 5]. In contrast to the $H_c$ behavior, the shape of the $H_{eb}$ is more notably changed for higher $H_U$ values; however, the distribution of the AF easy axes affects more visible the coercivity, as expected.[19]

The calculated angular variation of $H_{eb}$ shown in Fig. 5(a) is consistent with that obtained experimentally and numerically by Xi and White[35] for approximately the same $H_U$ and $H_E$ values as the ones used here. The $H_c$ variation calculated here for preferentially distributed AF anisotropy, however, fits their experimental data considerably better.

### C. Dependence of $H_{ra}$ on the coupling strength

As described in Sec. II, only the unstable AF grains contribute to the rotatable anisotropy due to the exchange interaction with the FM magnetization; the direction of this anisotropy coincides with the **H** direction. At a fixed temperature, the stronger the exchange coupling strength the larger the number of small AF grains whose magnetization vectors switch to stay close to the field direction. The $H_{ra}$ value is proportional to the sum of the projections of these magnetizations along **H**. Also, the stronger $H_E$ is the higher the values of these projections are. Hence the rotatable anisotropy should increase with the exchange coupling strength. As mentioned above, the coercivity for **H** applied along the exchange-bias direction is directly proportional to $H_{ra}$; thus $H_c$ should increase with $H_E$. Such a coercivity enhancement proportional to the exchange coupling between the FM and AF layers were observed experimentally by Leighton *et al.*[17] and also predicted by the SM model.[13]

### D. Temperature dependence of $H_c$

It was shown above that $H_c$ is strongly dependent on $H_E$ which decreases with the temperature increase. The coercivity, however, usually shows a well defined maximum in the vicinity of the blocking temperature, $T_B$, i.e., the temperature above which the exchange bias vanishes. Although in some cases $T_B \approx T_N$, where $T_N$ is the Néel temperature of the AF material, in other cases $T_B$ can be much lower than $T_N$ (see Refs. 3 and 40, and references therein). Coercivity peaks also appear in some model works, e.g., those of Fulcomer and Charap[8] and Stiles and McMichael.[13] This phenomenon is intuitively easy to understand by considering the temperature dependence of the AF grains. As $T_B$ is approached from below, their anisotropy is decreased and the reversal of the FM magnetization can induce more irreversible AF reorientations, thus increasing the FM coercivity. The latter reaches a maximum at the temperature for which all possible irreversible rotations are completed. For a further temperature increase, the coercivity variation follows that of $M_{AF}(T)$.

The maximum in the $H_c(T)$ curves can be very well explained from the temperature variation of $H_{ra}$, introduced in the present phenomenological model, and taking into account the corresponding variations of the other effective fields. Let us consider that the FM Curie temperature is much greater than $T_B$, i.e., the FM saturation magnetization and uniaxial anisotropy are temperature independent in the vicinity of $T_B$. If $M_{AF}(T) \propto (1-T/T_B)^{1/3}$ and assuming that the coupling field varies as the AF magnetization,[8] one obtains $H_E(T)=H_E(0)(1-T/T_B)^{1/3}$. As in the SM model, we used the expression $H_W(T)=H_W(0)(1-T/T_B)^{5/6}$ for the domain wall energy of the stable AF system, based on the assumption that the AF anisotropy constant $K_{AF}(T) \propto M_{AF}^3(T)$.

Only the AF grains that do switch their magnetizations for rotation of $\mathbf{M_{FM}}$ contribute to the rotatable anisotropy. One can express this as $H_{ra}(T)=H_{ra}(0)m(T)/m(0)$, where $H_{ra}(0)$ is the rotatable anisotropy at 0 K if the exchange field is so strong that the moments of all unstable AF are already rotated irreversibly, and $m$ is the magnetization of the small AF grain system scaled by its saturation value. Let us, for simplicity, assume that these grains are single-domain with effective anisotropy constant $K'_{AF}$ and they switch their magnetization through coherent rotation. The value of $K'_{AF}$ for these small grains, due to thermal activation, e.g., could be smaller than $K_{AF}$ of the larger grains. Also, as the interfacial coupling energy decreases with the increase of interface area of the grains,[13] the coupling constant for the small AF grains, $J'_1$, could be higher than that for the larger grains. At a fixed temperature, it is possible to calculate $m$; here this was done numerically in the framework of the Stoner–Wohlfarth model, assuming the same easy axis distribution for the small AF grains as the one used in Secs. III A and III B for the stable grains, and energy, $E'_{AF}$, which contains two terms,

$$E'_{AF}=-K'_{AF}t'_{AF}\left(\frac{\mathbf{M_{AF}}\cdot\hat{\mathbf{u}}_{\mathbf{AF}}}{M_{AF}}\right)^2-J'_1\frac{\mathbf{M_{FM}}\cdot\mathbf{M_{AF}}}{M_{FM}M_{AF}}, \qquad (6)$$

corresponding to the uniaxial anisotropy and the exchange interaction energies, respectively. Here $\mathbf{M_{FM}}$ is a constant vector lying along the external field direction. Thus the second term in this equation plays the role of the Zeeman term in the Stoner–Wohlfarth model. Taking into consideration that $K'_{AF}(T) \propto M_{AF}^3(T)$ and $J'_1(T) \propto H_E(T)$ [here, for simplicity, we assume that $J'_1(T) \approx J_1(T)$], one can calculate $m(T)$ and, consequently, the $H_{ra}(T)$ variation for the system of small interfacial AF grains.

With the help of $H_{ra}(T)$ thus obtained, and taking into account the variations with $T$ of the other effective fields, it is possible to calculate the hysteresis loops for the exchange-bias system at any temperature below $T_B$. Also, for $\phi_H=0$ and calculating the magnetization via the DWFra model, one can use the analytical expressions for $H_c$ derived in the framework of the DWF model[29] because, for **H** applied along the exchange-bias direction, the effective anisotropy

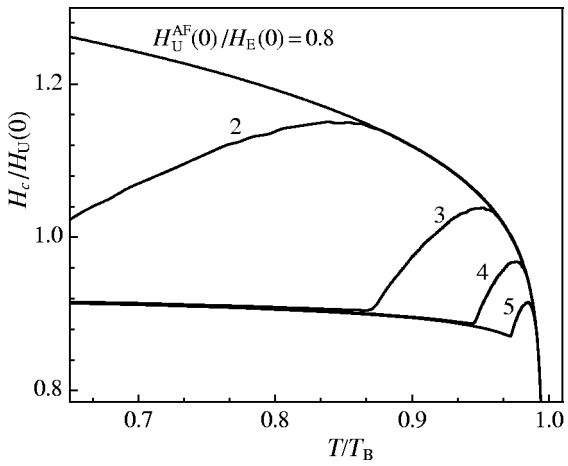


FIG. 6. Temperature dependence of $H_c$ for $\phi_H=0$ and for several representative values of $H_U^{AF}(0)/H_E(0)$, obtained through the DWFra model. The other parameters used in the calculations are $H_E(0)=60$ Oe, $H_W(0)=1.2$ kOe, $H_{ra}(0)=20$ Oe, and $H_U(0)=40$ Oe.

equals $H_{ra}+H_U$. For the case of weak interaction, i.e., $H_E(T)\ll H_W(T)$, the coercivity expression is[29]

$$H_c(T)=H_U+H_{ra}(T)+\frac{H_W(T)H_E^2(T)}{H_W^2(T)+H_E^2(T)}. \qquad (7)$$

The temperature dependences of the coercivity are plotted in Fig. 6 for five representative cases. For $H_U^{AF}(0)/H_E(0)>1$ (where $H_U^{AF}=2K'_{AF}/M_{AF}$), each curve shows a well expressed maximum below the blocking temperature, which broadens and moves towards lower temperatures upon decreasing the $H_U^{AF}(0)$ value, i.e., decreasing $K'_{AF}(0)/M_{AF}(0)$ or, alternatively, the size of the AF grains, if thermal activation effects are taken into account.

The maximum appears in $H_c(T)$ because there is a maximum in the $m(T)$ dependence. Actually, the existence of such a maximum in $m(T)$ is a manifestation of the so-called Hopkinson-type effect,[41] which can be observed for systems with uniaxial[42] as well as with cubic anisotropy.[43] Note that in the present model the Hopkinson effect is due to coherent magnetization rotations. However, if the mechanism for the magnetization changes in the small AF grains is domain wall motion, the effect is observed as well, the cause being the increase of the mobility of the domain wall with the temperature.[44] In both cases $H_{ra}(T)$, and as a consequence $H_c(T)$, show maxima provided that the exchange coupling field at the initial measuring temperature upon heating the sample is not sufficient to saturate *m*, which is the case of the curves for $H_U^{AF}(0)/H_E(0)>1$ plotted in Fig. 6.

In real samples, there is usually a spread of grain sizes, stress, interface coupling, etc., all of them influencing on $H_{ra}(T)$. Thus the shape of an experimentally obtained $H_c$ vs $T$ dependence may differ from these shown in Fig. 6.

## IV. SUMMARY

In this paper, we have described a phenomenological approach which explains the main features of the coercivity behavior of exchange-bias systems, i.e., the $H_c$ enhancement as compared to that of an uncoupled film, its variations with the exchange interaction strength, and its temperature dependence.

We model a FM film coupled to a polycrystalline AF layer consisting of two parts, one with rotatable and another with nonrotatable anisotropy. Small locally uncompensated interfacial AF grains, due to the exchange interaction with the FM magnetization, can switch their magnetizations irreversibly, thus producing effective rotatable anisotropy. Preferential distribution of the AF easy axes has also been considered; in such a case, it has been accepted that the FM film is divided into domains, each coupled to a stable AF grain, i.e., inhomogeneous reversal of the FM moments has been allowed.

The influence of the AF anisotropy distribution on the hysteresis loop shift, coercivity, and on the shape of the magnetization curves has been discussed, as well as their angular dependences. It was obtained that the distribution of the AF easy axes affects more visibly the coercivity, reducing its values in the vicinity of the exchange-bias direction, resulting in rounded $H_c$ vs $\phi_H$ curves; the $H_{eb}$ curves become smoother. These effects are more pronounced for small uniaxial anisotropy.

The inclusion of the rotatable anisotropy, in general, changes the shape of the magnetization curves as well as the $H_{eb}$ and $H_c$ values for fixed $\phi_H$. When the $H_U+H_{ra}$ value is small compared to that of $H_E$, the increase of $H_{ra}/(H_U+H_{ra})$ leads to a monotonic decrease of $H_{eb}$. For higher $H_U+H_{ra}$ values, however, neither the $H_{eb}$ nor $H_c$ variations with $H_{ra}$ are simple.

If the value of $H_U+H_{ra}$ is kept fixed while $H_{ra}$ is varied, the relative $H_{ra}$ increase generates smoother $H_{eb}$ vs $\phi_H$ curves, whose behavior becomes very close to pure $\cos 2\phi_H$ for a strong AF anisotropy. This effect is similar to that caused by the increase of the exchange coupling strength. The rotatable anisotropy does almost not affect the coercivity if the coupling is strong.

As the $H_{ra}$ value is proportional to the magnetization of the small AF grains, it increases with the coupling strength. Thus, for a field applied along the exchange-bias direction, $H_c$ increases with $H_E$ as well.

The frequently observed broad peak in the temperature variation of $H_c$ in the vicinity of the AF blocking temperature has been explained from the temperature variation of $H_{ra}$. The latter shows a maximum upon heating because there is a maximum in the corresponding temperature dependence of the magnetization of the small AF grains, if the coupling field is not high enough to saturate this system at the initial measuring temperature.

## ACKNOWLEDGMENTS

We thank J. Nogués for a critical reading of the paper. This work was supported by the Conselho Nacional de Desenvolvimento Científico e Tecnológico (CNPq, Brazil) and the Fundação de Amparo à Pesquisa do Estado do Rio Grande do Sul (FAPERGS, Brazil).

*Electronic address: julian@if.ufrgs.br

[1] W. H. Meiklejohn and C. P. Bean, Phys. Rev. **102**, 1413 (1956); **105**, 904 (1957).
[2] W. H. Meiklejohn, J. Appl. Phys. **33**, 1328 (1962).
[3] J. Nogués and Ivan K. Schuller, J. Magn. Magn. Mater. **192**, 203 (1999).
[4] A. E. Berkowitz and K. Takano, J. Magn. Magn. Mater. **200**, 552 (1999).
[5] R. L. Stamps, J. Phys. D **33**, R247 (2000).
[6] B. Dieny, V. S. Speriosu, S. S. P. Parkin, B. A. Gurney, D. R. Wilhoit, and D. Mauri, Phys. Rev. B **43**, 1297 (1991).
[7] B. Dieny, A. Granovsky, A. Vedyaev, N. Ryzhanova, C. Comanche, and L. G. Pereira, J. Magn. Magn. Mater. **151**, 378 (1995).
[8] E. Fulcomer and S. H. Charap, J. Appl. Phys. **43**, 4190 (1972).
[9] A. P. Malozemoff, Phys. Rev. B **35**, 3679 (1987).
[10] D. Mauri, H. C. Siegmann, P. S. Bagus, and E. Kay, J. Appl. Phys. **62**, 3047 (1987).
[11] B. H. Miller and E. D. Dahlberg, Appl. Phys. Lett. **69**, 3932 (1996).
[12] Z. Qian, J. M. Sivertsen, and J. H. Judy, J. Appl. Phys. **83**, 6825 (1998).
[13] M. D. Stiles and R. D. McMichael, Phys. Rev. B **59**, 3722 (1999); **60**, 12 950 (1999); **63**, 064405 (2001).
[14] M. Kiwi, J. Mejía-López, R. D. Portugal, and R. Ramírez, Europhys. Lett. **48**, 573 (1999); Appl. Phys. Lett. **75**, 3995 (1999); Solid State Commun. **116**, 315 (2000).
[15] H. Xi and R. M. White, Phys. Rev. B **61**, 80 (2000).
[16] Z. Li and S. Zhang, Phys. Rev. B **61**, R14 897 (2000).
[17] C. Leighton, J. Nogués, B. J. Jösson-Åkerman, and Ivan K. Schuller, Phys. Rev. Lett. **84**, 3466 (2000).
[18] C. Hou, H. Fujiwara, and F. Ueda, J. Magn. Magn. Mater. **198-199**, 450 (1999).
[19] T. Zhao, H. Fujiwara, K. Zhang, C. Hou, and T. Kai, Phys. Rev. B **65**, 014431 (2001).
[20] J. Sort, J. Nogués, X. Amils, S. Suriñach, J. S. Muñoz, and M. D. Baró, Appl. Phys. Lett. **75**, 3177 (1999); J. Sort, J. Nogués, S. Suriñach, J. S. Muñoz, M. D. Baró, E. Chappel, F. Dupont, and G. Chouteau, Appl. Phys. Lett. **79**, 1142 (2001).
[21] R. D. McMichael, M. D. Stiles, P. J. Chen, and W. F. Egelhoff, Jr., Phys. Rev. B **58**, 8605 (1998).
[22] P. Lubitz, J. J. Krebs, M. M. Miller, and S.-F. Cheng, J. Appl. Phys. **83**, 6819 (1998).
[23] M. Rubinstein, P. Lubitz, and S.-F. Cheng, J. Magn. Magn. Mater. **195**, 299 (1999); **210**, 329 (2000).
[24] V. Ström, B. J. Jönsson, and E. D. Dahlberg, J. Appl. Phys. **81**, 5003 (1997).
[25] P. Miltényi, M. Gruyters, G. Güntherodt, J. Nogués, and Ivan K. Schuller, Phys. Rev. B **59**, 3333 (1999).
[26] H. Xi, R. M. White, and S. M. Rezende, Phys. Rev. B **60**, 14 837 (1999).
[27] J. R. Fermin, M. A. Lucena, A. Azevedo, F. M. de Aguiar, and S. M. Rezende J. Appl. Phys. **87**, 6421 (2000).
[28] E. D. Dahlberg, B. Miller, B. Hill, B. J. Jönsson, V. Ström, K. V. Rao J. Nogués, and Ivan K. Schuller, J. Appl. Phys. **83**, 6893 (1998).
[29] J. Geshev, Phys. Rev. B **62**, 5627 (2000).
[30] J. Geshev, L. G. Pereira, and J. E. Schmidt, Phys. Rev. B **64**, 184411 (2001).
[31] R. J. Prosen, J. O. Holmen, and B. E. Gran, J. Appl. Phys. **32**, 91S (1961).
[32] F. Nolting, A. Scholl, J. Stöhr, J. W. Seo, J. Fompeyrine, H. Siegwart, J.-P. Locquet, S. Anders, J. Lüning, E. E. Fullerton, M. F. Toney, M. R. Scheinfein, and H. A. Padmore, Nature (London) **405**, 767 (2000).
[33] D. J. Webb and S. M. Bhagat, J. Magn. Magn. Mater. **42**, 121 (1984).
[34] B. D. Cullity, *Introduction to Magnetic Materials* (Addison-Wesley, London, 1972).
[35] H. Xi and R. M. White, J. Appl. Phys. **86**, 5169 (1999).
[36] D. V. Dimitrov, S. Zhang, J. Q. Xiao, G. C. Hadjipanayis, and C. Prados, Phys. Rev. B **58**, 12 090 (1998).
[37] J. Nogués, D. Lederman, T. J. Moran, and I. K. Schuller, Phys. Rev. Lett. **76**, 4624 (1996).
[38] T. Ambrose, R. L. Sommer, and C. L. Chien, Phys. Rev. B **56**, 83 (1997).
[39] N. L. Gökemeijer, T. Ambrose, and C. L. Chien, Phys. Rev. Lett. **79**, 4270 (1997).
[40] C. Leighton, M. R. Fitzsimmons, A. Hoffmann, J. Dura, C. F. Majkrzak, M. S. Lund, and Ivan K. Schuller, Phys. Rev. B **65**, 064 403 (2002).
[41] J. Hopkinson, Proc. R. Soc. London, Ser. A XLVIII, 1 (1890).
[42] O. Popov and M. Mikhov, J. Magn. Magn. Mater. **75**, 135 (1988); **82**, 29 (1989).
[43] J. Geshev, O. Popov, V. Masheva, and M. Mikhov, J. Magn. Magn. Mater. **92**, 185 (1990).
[44] M. Kersten, Z. Angew. Phys. **8**, 313 (1956).